Reusing of transmitted light by localized surface plasmon enhancing of Ag nanoparticles in organic solar cells*

WANG Chao(王超), **QIN Wen-jing**(秦文静)**, **MA Chun-yu**(马春宇), **ZHANG Qiang**(张强), **YANG Li-ying**(杨利营), **and YIN Shou-gen**(印寿根)**

Key Laboratory of Display Materials and Photoelectric Devices, Education Ministry of China, Tianjin Key Laboratory for Photoelectric Materials and Devices, School of Materials Science and Engineering, Tianjin University of Technology, Tianjin 300384, China

(Received 9 August 2012)

Silver nanoparticles (Ag NPs) are synthesized with chemical method, which are introduced into the traditional organic photovoltaic (OPV) structure. The experimental results show that both the optical and photoelectric properties are enhanced because of localized surface plasmon (LSP) effects of Ag NPs. The advantage of adding Ag NPs behind active layer in incident direction is discussed. We believe this route can avoid absorption shadow and enhance the reusing of transmitted light of active layer. The average short-circuit current (J_{SC}) of the optimum device can be raised from 9.23 mA/cm^2 to 10.84 mA/cm^2, and the energy converting efficiency (PCE) can be raised from 3.22% to 3.85%.

Document code: A **Article ID:** 1673-1905(2012)06-0401-4

DOI 10.1007/s11801-012-2326-2

With the advantages of low cost, easy fabrication, flexible and foldable structure, organic photovoltaics (OPV) can have the vital significance to large-scale use of solar energy to obtain cheap and safe electricity[1]. However, the limited light absorption and low carrier mobilities of organic materials cause mismatch between the best absorption thickness of active layer (100 nm) and the exciton diffusion length (10 nm)[2,3]. In order to enhance the light absorbance without increasing the thickness of active layers, researchers have developed many strategies, such as tandem cells[4], diffraction grating[5] and dye sensitization[6]. Recent years, the surface plasmon polariton The SPP[7] was introduced in the research work of the OPV. The SPP is an electromagnetic excitation existing on surface of a noble metal. At first, electromagnetic field is enhanced by incident light, which is passing through specific sub-wavelength structure. And then, by coupling with incident light, the field can trap more light and promote the generation and separation of excitons. In 1996, Stuart and Hall[8] introduced silver nanoparticles (Ag NPs) into the amorphous silicon thin film photovoltaic cells, forming metal islands like film to stimulate localized surface plasmon (LSP) and improve the photocurrent for the first time. Since then, stimulating LSP using metal nanoparticles is widely used in OPV performance optimization[9,10].

At present, scientists have applied many kinds of preparation methods[11,12], and studied the influence of metal structure with different parameters on photovoltaic performance. The studies improved the light absorbance and the photoelectric performance of OPV in different ways[13]. Meanwhile, the influence factors for plasmon enhanced OPV performance were studied, such as metal structure sizes[14], densities[15] and periodicities[11,12]. But these researchers mainly studied SPP effect on transmission enhancement by incorporating the metal structure, which is usually before the active layer in the light incidence direction. It generally requires a strict control over the size, density and periodicity of metal structure. Otherwise, it can cause absorption shadow, and decrease the absorption of active layer. Placing the metal structure behind the active layer is a viable way to solve this problem. But physical method didn't adapt for the traditional device assemble process. No systematic research has been performed to investigate the optimum parameters of metal structure behind active layer.

In this paper, Ag NPs are added behind active layer in

* This work has been supported by the National Natural Science Foundation of China (Nos.60876046 and 60976048), the Tianjin Natural Science Foundation (Nos.10ZCKFGX01900, 10SYSYJC28100 and 12JCQNJC01300), the Scientific Developing Foundation of Tianjin Education Commission (No.20100723), and the Tianjin Key Discipline of Material Physics and Chemistry.

** E-mails: qinerrrr@yahoo.com.cn; sgyin@tjut.edu.cn

incident direction. By ruling out the disturbance of absorption shadow, the light scattering from metal nanoparticles and the light coupling effect of SPP are studied absolutely. The influence of Ag NPs on the absorption of active layer is investigated, and the optical-electrical performance is improved finally.

Ag NPs were synthesized with the liquid-solid-solution (LSS) strategy. 10 mL of silver nitrate solution (0.025 g/mL), 2 mL of oleic acid, 0.8 g of sodium oleate and 20 mL of ethanol were added into a 50 mL autoclave, and then heated at 90 °C for 10 h. After cooling to room temperature, dark brown precipitate was obtained at the bottom of autoclave. Centrifugally clean the precipitate with ethanol repeatedly after pouring out the clear liquid, and then disperse the precipitate in ethanol.

The schematic diagrams of OPVs' structures are shown in Fig.1. First, PEDOT:PSS buffer layer (~30 nm) and P3HT:PCBM active layer (~120 nm) were spin-coated onto ITO substrate. The heat treatments are in vacuum at 110 °C for 1 h and in vacuum at 140 °C for 15 min, respectively. Then, spin the Ag NPs ethanol dispersion onto ITO substrate at 800 r/min for 12 s to form monolayer scattered Ag NPs film, and evaporate the solvent in vacuum oven at 60 °C for 5 min, so multi-layer scattered Ag NPs can be obtained through repeated spin coating. Devices with 1−5 layers of Ag NPs are named as S1 to S5, and the traditional device of control experiment is short for CD. At last, 1 nm of LiF modify layer and 15 nm of Al cathode layer were thermal-evaporation deposited by order.

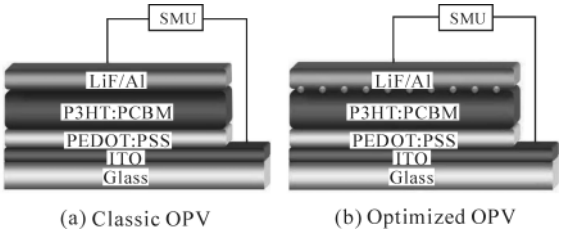

Fig.1 Schematic diagrams of OPVs' structures

The morphologies and surface topographies of films were measured with JEOL® JSM-7001F scanning electron microscopy (SEM) and JEOL® JEM-2100 transmission electron microscopy (TEM). The absorption spectra were measured with Hitachi U-4100 ultraviolent-visible (UV-VIS) spectrophotometer. The crystal structure characteristics of powder were measured with Rigaku® D/MAX-2500 v/PC X-ray diffraction (XRD). Current density versus voltage (*J-V*) curves were measured with a Keithley 2400 source meter under 100 mW/cm^2 (AM1.5G) illumination from Newport® 94021a-1000 at room temperature in atmosphere. Monochromatic incident photon-to-electron conversion efficiency (IPCE) was measured with Crowntech® IPCE measuring system made up of 1/4 monochromator QEM-24-S and integrating spheres CT-IS-004. Work function of thin film was calibrated with KP020 Kelvin Probe.

Fig.2(a) is the XRD figure of precipitation powder, and the insert is the TEM image. XRD shows the diffraction peaks of the sample match with face-centered cubic silver (JCPDS (No.-0783)) perfectly, corresponding to the Ag (111), Ag (200), Ag (220) and Ag (311), respectively. No obvious miscellaneous peak exists, which proves that the sample is silver with high purity. Calculated by Scherrer formula, the average particle size of Ag NPs is about 23.82 nm, which matches the TEM images. By repeated spin-coating, scattered Ag NPs films with different densities were fabricated, and the SEM images are shown in Fig.2(b)-(f). As can be seen from Fig.2(b)-(f), Ag NPs are dispersed well. With the times of spin coating increase, the Ag NPs densities grow gradually, and the values are ~18 /μm^2 for 1 layer, ~25 /μm^2 for 2 layers, ~50 /μm^2 for 3 layers, ~100 /μm^2 for 4 layers, ~250/μm^2 for 5 layers.

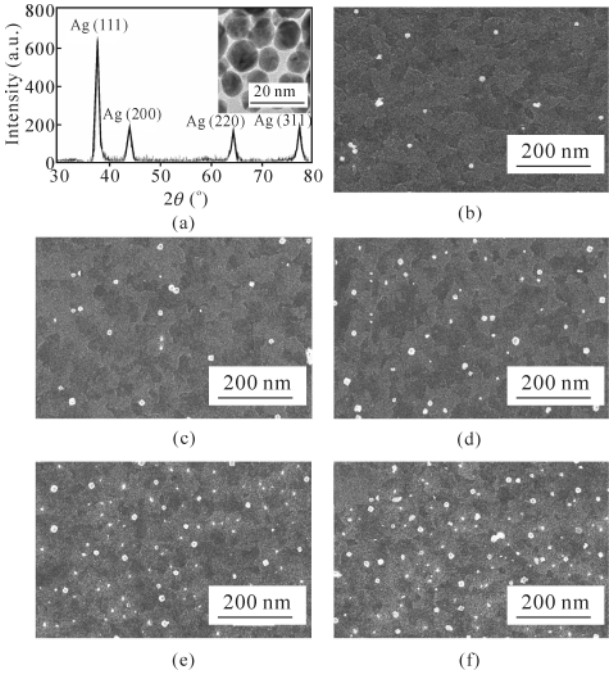

Fig.2 Crystal structure and morphology of Ag NPs: (a) XRD peaks of silver nano powder (The inset is TEM of Ag NPs); (b)-(f) SEM images of scattered Ag NPs films spin coated on ITO with 1-5 layers

In order to evaluate the influence of the Ag NPs with different densities to the P3HT:PCBM active layer on its absorbance, the UV-VIS absorption spectra of the classic devices and optimized ones are measured, as shown in Fig.3(a). It reveals that with Ag NPs, the active layer makes absorbance enhanced in the range from 350 nm to 650 nm, which results from LSP effect[16]. After surface plasmon around the surface

of Ag NPs is stimulated, incident light can be coupled in very broad spectrum range and stimulate LSP effect. According to Mie theory[17], when the radius of particle meets

$$a \le \frac{0.3\lambda}{2\pi} \quad , \tag{1}$$

incident light can be Rayleigh scattered by the particle, and make the scattering light have the same wavelength as incident light. As the Ag NPs are far smaller than the incident light wavelength, according to Rayleigh scattering condition, incident light can be trapped and then scattered into any direction. At the same time, light at the media interface is scattered asymmetrically, and the light scatters preferentially into the active layer with the larger permittivity which effectively increases the optical path length[18]. Thus, the reusing of light is enhanced significantly, and the absorbance of active layer is improved.

With the increasing of Ag NPs' density, the absorbance of the devices is increased, which also accords with the LSP light coupling. According to the Mie theory, the interaction between incident photons and the plasmonics follows the Maxwell's equations of nanoparticles' internal absorption and external scattering electromagnetic field. From its primary solution, the absorption/scattering cross section $\sigma(\omega)$ is obtained[19,20] as

$$\sigma(\omega) = \frac{9N\omega V\varepsilon_s^{3/2}}{c}\left\{\frac{\varepsilon_2(\omega)}{\left[\varepsilon_1(\omega)+2\varepsilon_2(\omega)\right]^2+\varepsilon_2^2(\omega)}\right\} \quad , \tag{2}$$

where N is the bulk density of nanoparticles, $\omega = 2\pi/\lambda$ is the frequency of incident electromagnetic field, ε_S is the dielectric constant of surrounding media, V is the volume of nanoparticle, c is the speed of light in vacuum, and ε_1 and ε_2 are the real part and imaginary part of metal dielectric constant, also known as external scattering and internal absorption of metal nanoparticles.

$$\left[\varepsilon_1(\omega)+2\varepsilon_2(\omega)\right]^2+\varepsilon_2^2(\omega)=0 \tag{3}$$

is Mie scattering resonance condition[20]. When ω meets Eq.(3), its value is called as Mie resonance frequency, and the section area of the interaction between incident light and nanoparticles is far greater than the geometry area of the nanoparticles. Thus, a bigger plasma field is stimulated to make the incident light bound into medium material, and light absorbance of the medium is enhanced. Then Eq.(2) can be simplified as

$$\sigma(\omega) \propto N \, . \tag{4}$$

Predictably, in our experiment, the higher the Ag NPs' density is, the greater the absorption-scattering section area is, and the more greatly the electromagnetic field is enhanced, which results in capturing more photons.

The LSP effects on photovoltaics are studied through evaluating the photoelectric performance of control device and the optimized devices, which are shown in Fig.3(b)-(d). Fig.3(b) lists the IPCE curves for devices S1-S4. The enhancement trends of their IPCEs are the same as their absorption enhancement trends; but for device S5, its IPCE is decreased with the growth of absorbance. This phenomenon can be explained based on the variation of interface potential energy barrier, and the work functions of these Ag NPs layers are 4.6−4.8 eV, which enlarge the energy barrier between LUMO (4.2 eV) and HOMO (4.3 eV) of the PCBM used in this paper, and narrow the electronic transmission channel. With the density of Ag NPs increasing, the channel for electrons transport to the cathode becomes narrower; and for the device coated with 5 layers of Ag NPs, electrons transport blocking effect inside device takes the advantage of LSP enhancement effect, so the output of device is lowered.

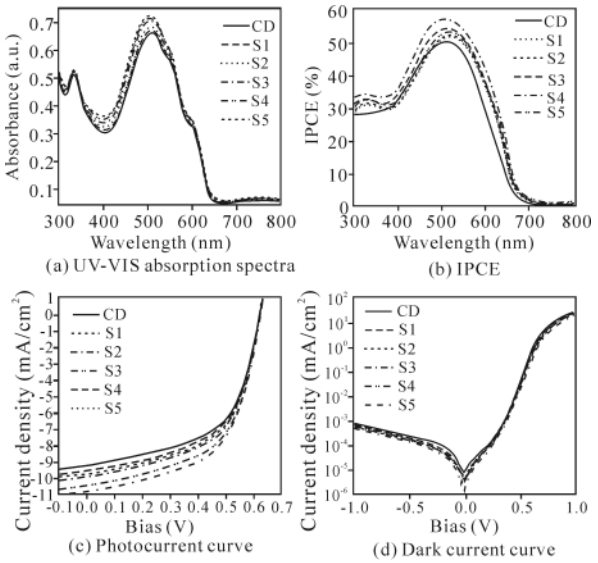

Fig.3 Optical and photoelectric properties of OPVs

Tab.1 shows the open-circuit voltages (V_{OC}), short-circuit current densities (J_{SC}), PCE, fill factors (*FF*) and series resistances (R_S) of the OPV devices, which are calculated from the photocurrent curve in Fig.3(c). Compared with CD, the V_{OC} of the optimized devices changes little after adding Ag NPs. One important reason for that is that the interface energy barrier between P3HT and PCBM, which is the dominant factor impacting the V_{OC}, is not changed in optimized devices; the other key factor impacting V_{OC} is the diode characteristics of OPV device[21,22]. Dark *J*-*V* curve in Fig.3(d) shows that the optimized devices have relatively stable commutating ratios at 10^5, which indicates that their diode characteristics do not change significantly. Thus, the V_{OC} of the optimized devices changes little.

Tab.1 Photoelectric performance parameters of OPV devices

	V_{OC} (V)	J_{SC} (mA/cm^2)	*PCE* (%)	*FF* (%)	R_S (Ω • cm^2)
CD	0.62(±0.01)	9.23(±0.03)	3.22(±0.06)	56.27(±0.69)	10.62(±0.18)
S1	0.62(±0.01)	9.59(±0.07)	3.35(±0.08)	56.34(±0.95)	8.68((±0.21)
S2	0.62(±0.01)	9.93(±0.09)	3.47(±0.09)	56.36(±0.92)	8.99(±0.21)
S3	0.62(±0.01)	10.47(±0.11)	3.68(±0.15)	56.69(±0.66)	9.96(±0.18)
S4	0.62(±0.01)	10.84(±0.08)	3.85(±0.06)	57.28(±0.85)	9.48(±0.20)
S5	0.62(±0.01)	9.76(±0.23)	3.41(±0.21)	56.35(±1.05)	10.59(±0.23)

The J_{SC} has the same variation tendency as IPCE, and is raised from 9.23 mA/cm^2 to 10.84 mA/cm^2, which is increased by 17% compared with the control device. And with the further increase of Ag NPs' density, the J_{SC} decreases instead. It is because the photocurrent is relevant to the generation and transmission of photocarriers. On one hand, LSP on the surface of Ag NPs couples the transmitted photons and converts them to excitons in active-layer. Meanwhile, the segregation rate of photo-generated excitons is improved by LSP resonance field to generate more carriers, so the photocurrent is enhanced. On the other hand, too high density of Ag NPs enlarges the interface barrier of electron path, and some low-energy electrons cannot arrive at cathode, so the photocurrent can be lowered. As a result of the contradiction between electron generation improvement and the transmission obstacle, J_{SC} decreases after reaching its optimum value.

The *FF* is increased slightly, but the R_s changes irregularity. We deduce that excitation of the LSP increases the rate of exciton generation and dissociation. But the interface energy barrier is enlarged with incorporating Ag NPs[22,23], so the variation of *FF* is not obvious. As a result, only the factor of J_{SC} can determine the optimization result of PCE. The optimum PCE is raised from 3.22% to 3.85%, and gets an increase amplitude of 20%.

Ag NPs layers are added in OPV devices behind the active layer, which makes transmitted light coupled, LSP stimulated, the energy of transmitted light transferred to the active layer, and more excitons generated. Meanwhile, the LSP resonance field improves the segregation rate of photo-generated excitons. But in the process of charge carriers transmitting to the cathode, too high density of Ag NPs blocks the transmission, and makes the photocurrent descend. The device with Ag NPs spin-coated for four times is the optimum one, whose J_{SC} is increased by 17%, and its PCE is improved by 20%.

References

[1] G. Yu, J. Gao, J. C. Hummelen, F. Wudl and A. J. Heeger, Science **270**, 1789 (1995).

[2] L. M. Chen, Z. Hong, G. Li and Y. Yang, Advanced Materials **21**, 1434 (2009).

[3] R. Po, M. Maggini and N. Camaioni, Journal of Physical Chemistry C **114**, 695 (2009).

[4] Jin Young Kim, Kwanghee Lee, Nelson E. Coates, Daniel Moses, Thuc-Quyen Nguyen, Mark Dante and Alan J. Heeger, Science **317**, 222 (2007).

[5] C. Cocoyer, L. Rocha, L. Sicot, B. Geffroy, R. de Bettignies, C. Sentein, C. Fiorini-Debuisschert and P. Raimond, Applied Physics Letters **88**, 133108 (2006).

[6] HE Zu-ming, XIA Yong-mei, WANG Qing and ZHANG Xiao-nan, Journal of Optoelectronics • Laser **22**, 219 (2011). (in Chinese)

[7] H. Raether, Surface Plasmons, Springer-Verlag Berlin, 1988.

[8] H. R. Stuart and D. G. Hall, Applied Physics Letters **69**, 2327 (1996).

[9] F. Beck, A. Polman and K. Catchpole, Journal of Applied Physics **105**, 114310 (2009).

[10] Linfang Qiaoa, Dan Wanga, Lijian Zuob, Yuqian Yea, Jun Qiana, Hongzheng Chenb and Sailing He, Applied Energy **88**, 848 (2010).

[11] X. Chen, C. Zhao, L. Rothberg and M. K. Ng, Applied Physics Letters **93**, 123302 (2008).

[12] Seok-Soon Kim, Seok-In Na, Jang Jo, Dong-Yu Kim and Yoon-Chae Nah, Applied Physics Letters **93**, 073307 (2008).

[13] LI Hai-jun, ZHANG Xiao-dong, WANG Min-rui, LIN Wen-kui, SHI Wen-hua, ZHONG Fei and ZHANG Bao-shun, Optoelectronics Letters **6**, 211 (2010).

[14] Qingbo Zhang, Jianping Xie, Jinhua Yang and Jim Yang Lee, ACS Nano **3**, 139 (2008).

[15] Woo-Jun Yoona, Kyung-Young Junga, Jiwen Liub, Thirumalai Duraisamyb, Rao Revurb, Fernando L. Teixeiraa, Suvankar Senguptab and Paul R. Berger, Solar Energy Materials and Solar Cells **94**, 128 (2010).

[16] J. Bellessa, C. Bonnand, J. C. Plenet and J. Mugnier, Physic al Review Letters **93**, 36404 (2004).

[17] P. Kik and M. Brongersma, Springer Series in Optical Sciences **31**, 1 (2007).

[18] T. D. Heidel, J. K. Mapel, M. Singh, K. Celebi and M. A. Baldo, Applied Physics Letters **91**, 093506 (2007).

[19] D. Duchea, P. Torchioa, L. Escoubasa, F. Monestiera, J.-J. Simona, F. Floryb and G. Mathian, Solar Energy Materials and Solar Cells **93**, 1377 (2009).

[20] D. D. Evanoff Jr and G. Chumanov, Journal of Physical Chemistry B **108**, 13957 (2004).

[21] C. J. Brabec, A. Cravino, D. Meissner, N. S. Sariciftci, T. Fromherz, M. T. Rispens, L. Sanchez and J. C. Hummelen, Advanced Functional Materials **11**, 374 (2001).

[22] B. P. Rand, D. P. Burk and S. R. Forrest, Physical Review B **75**, 115327 (2007).

[23] A. Gadisaa, F. Zhang, D. Sharma, M. Svensson, M. R. Andersson and O. Inganäs, Thin Solid Films **515**, 3126 (2007).